



## Featured Letter

# Microwave-assisted synthesis of palladium nanoparticles using *Frankincense* resin and evaluation of their catalytic properties



Kondaiah Seku<sup>a</sup>, Syed Sulaiman Hussaini<sup>a</sup>, Narasimha Golla<sup>b</sup>, Girija Mangatayaru K<sup>c</sup>, Sri Maha Vishnu D<sup>d</sup>, Sridhar Rapolu<sup>e</sup>, Rajkumar Bandi<sup>f</sup>, Bhagavanth Reddy G<sup>c,\*</sup>

<sup>a</sup> Department of Chemistry, Shinas College of Technology, Shinas, Sultanate of Oman

<sup>b</sup> Department of Virology, Sri Venkateshwara University, Tirupati, India

<sup>c</sup> Department of Chemistry, Palamuru University, Mahbubnagar, Telangana, India

<sup>d</sup> Department of Materials Science and Metallurgy, University of Nizwa, Birkat Al Mouz, Nizwa, Oman

<sup>e</sup> Department of Basic Science and Humanities, Vignan Institute of Technology and Science, Telangana, India

<sup>f</sup> Department of Chemistry, Osmania University, Hyderabad, India

## ARTICLE INFO

## Article history:

Received 3 June 2020

Received in revised form 13 July 2020

Accepted 28 July 2020

Available online 31 July 2020

## Keywords:

*Frankincense* resin

Palladium nanoparticles

Organic pollutants

Recyclable catalyst

## ABSTRACT

The present study describes a microwave-assisted synthesis of well-dispersed palladium nanoparticles (PdNPs). For the first time, *Frankincense* resin (FR) obtained from the tree of *Boswellia sacra* is explored for the preparation of PdNPs. This method is rapid, inexpensive and devoid of toxic chemicals. FR aqueous extract with reducing polysaccharides and other phytochemicals served as an effective reducing and stabilizing agent for PdNPs. Formation of PdNPs was preliminarily confirmed by UV-visible and mechanism of formation was proposed from Fourier transform infrared spectroscopy. Transmission electron microscopic images displayed spherical PdNPs with an average size of  $11 \pm 2$  nm. Catalytic activity studies revealed that the PdNPs act as an efficient catalyst for the reduction of both cationic (Methylene Blue) and anionic (Congo red) dye pollutants. Moreover, the PdNPs can be recovered and reused for five cycles without a significant loss in their catalytic activity.

© 2020 Elsevier B.V. All rights reserved.

## 1. Introduction

Palladium nanoparticles (PdNPs) grabbed great attention from the scientific community with their vast applications in catalysis, coatings, plastics, textiles, fuel cells, sensor design and active membranes [1,2,3]. With this great demand, so far numerous physical and chemical methods have been developed for the production of PdNPs [4,5]. However, high operational cost and/or usage of hazardous chemicals that can pose potential threat to the environment and various forms of life are the downsides [6,7]. In this context, developing inexpensive and harmless methods for the PdNPs preparation is blooming [4]. *Frankincense* resin (FR) is a naturally occurring gum resin obtained as an exudate from the bark of *Boswellia sacra* a native tree of Sultanate of Oman [8]. Characteristically FR contains phytochemicals such as polysaccharides, essential oils, proteins, and terpenoids which can efficiently reduce Pd(II) ions to PdNPs, control their growth and protect them from aggregation [6]. More importantly FR is cheap, renewable and non-toxic. Furthermore, in comparison with the conventional heat

treatment, microwave irradiation (MWI) is promising with homogenous heating that produces rapid nucleation, uniform and small sized particles [9]. Hence, this work explores the usage of FR for the production of PdNPs by MWI method and evaluates the catalytic activity of the formed PdNPs.

## 2. Experimental section

1 g of FR (finely powdered) was mixed with 100 mL of double distilled water in a beaker. The solution was heated at 60 °C for 6 h, cooled to room temperature and filtered through the Whatman filter paper to get a clear resin solution. About 5 mL of 1 mM Na<sub>2</sub>-PdCl<sub>4</sub> solution was mixed with 10 mL of 0.5% resin extract in a beaker. The reaction mixture was exposed to MWI at 450 W for 5 min. The resulting grey colored PdNPs solution was centrifuged, washed and dried to get PdNPs powder. The absorption spectra were recorded on UV-Visible spectrophotometer (Shimadzu UV-3600). Fourier transform infrared (FT-IR) spectra recorded on IRAffinity-1, Shimadzu, X-ray diffraction (XRD) analysis was conducted on Rigaku-Miniflex and Transmission electron microscope (TEM) images were acquired on JEOL 2000FX-II. Procedure for the reduction of dyes can be found in [supporting information](#) (SI).

\* Corresponding author.

E-mail address: [bhagavanth.g@gmail.com](mailto:bhagavanth.g@gmail.com) (B. Reddy G).

### 3. Results and discussion

Upon MWI, the pale yellow colored reaction mixture turned black indicating the formation of PdNPs. The UV–Vis spectra of the reactants and product are shown in Fig. 1a. It is well known that the intensity of the characteristic absorption peaks of Pd(II) precursor will decrease after its reduction to Pd(0) [6]. Hence the MWI is continued until the complete disappearance of characteristic peaks (300 & 425 nm) and 5 min of MWI time is selected as optimum. XRD pattern (Fig. 1c) presented four peaks (39.65°, 45.24°, 65.14°, and 78.65°) respectively corresponding to (111), (200), (222) and (311) diffractions of the face centered cubic (FCC) crystal structure of elemental Pd (JCPDS No. 89 – 4897) [4] which revealed the high crystallinity of the PdNPs. High intensity of (111) peak indicates the preferential growth of Pd nanocrystals along this plane and the average crystallite size calculated from (111) peak using Scherrer formula [9] was found to be 9.1 nm. The TEM image of PdNPs is shown in Fig. 1d. Most of the particles are spherical in shape with an average size of  $11 \pm 2$  nm and very few particles differ in their shape and size.

The possible mechanism for the synthesis of PdNPs using FR involves two steps. Initially Pd(II) will undergo complexation with hydroxyl and carbonyl functions of various phytochemicals present in FR. Due to the strong antioxidant nature and high reducing

capacity, these hydroxyl and carbonyl functions will reduce Pd(II) to Pd(0) atoms and undergo oxidation to carboxyl groups. Pd atoms serve as nucleation sites for the growth of PdNPs. Finally, the size control and stabilization of PdNPs is achieved by the surface coating of these phytochemicals through binding interactions between metal atoms and oxygen containing functional groups. This hypothesis was verified by FTIR analysis of FR before and after PdNPs synthesis (Fig. 1c). Decrease in the intensity of peaks related to hydroxyl and carbonyl groups and appearance of new peak corresponding to carboxyl clearly demonstrate that hydroxyl and carbonyl groups are responsible for synthesis and stabilization process of PdNPs [10]. Complete details on FTIR analysis is provided in SI.

Catalytic activity of PdNPs was assessed by performing NaBH<sub>4</sub> mediated degradation of organic dye pollutants. Methylene blue (MB) and Congo red (CR) were selected as model cationic and anionic dyes respectively. Fig. 2a depicts the UV–Visible absorption spectrum of CR dye, that shows two absorption bands at 345(n- $\pi^*$ ) and 500 nm( $\pi$ - $\pi^*$ ) characteristic to azo group [9]. In the presence of NaBH<sub>4</sub> alone, no obvious change in the peak intensity is observed even after 120 min (Fig. S1), signifying the need of catalyst. After the introduction of PdNPs into the reaction mixture, a swift decline in the peak intensity was observed, the reduction was completed within 150sec. The efficiency of CR reduction was

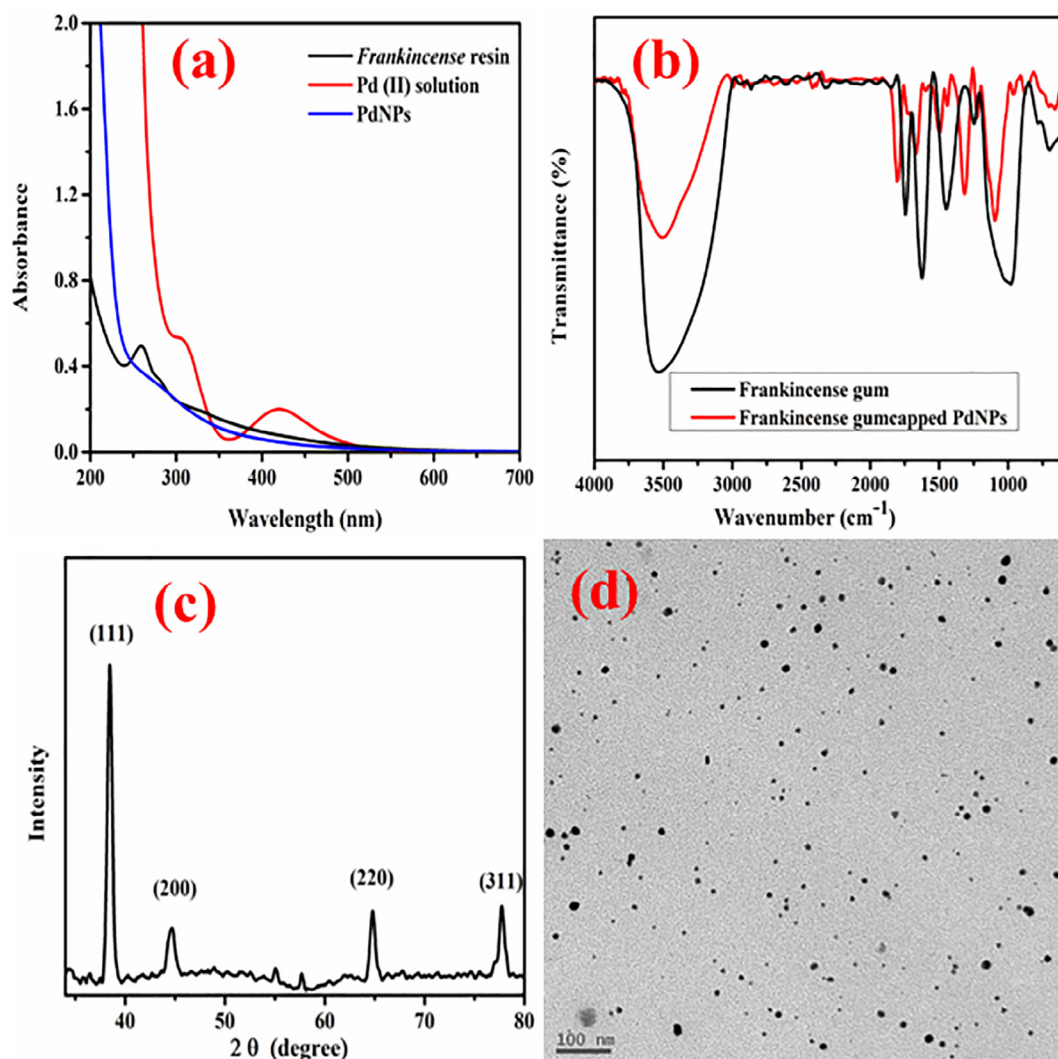
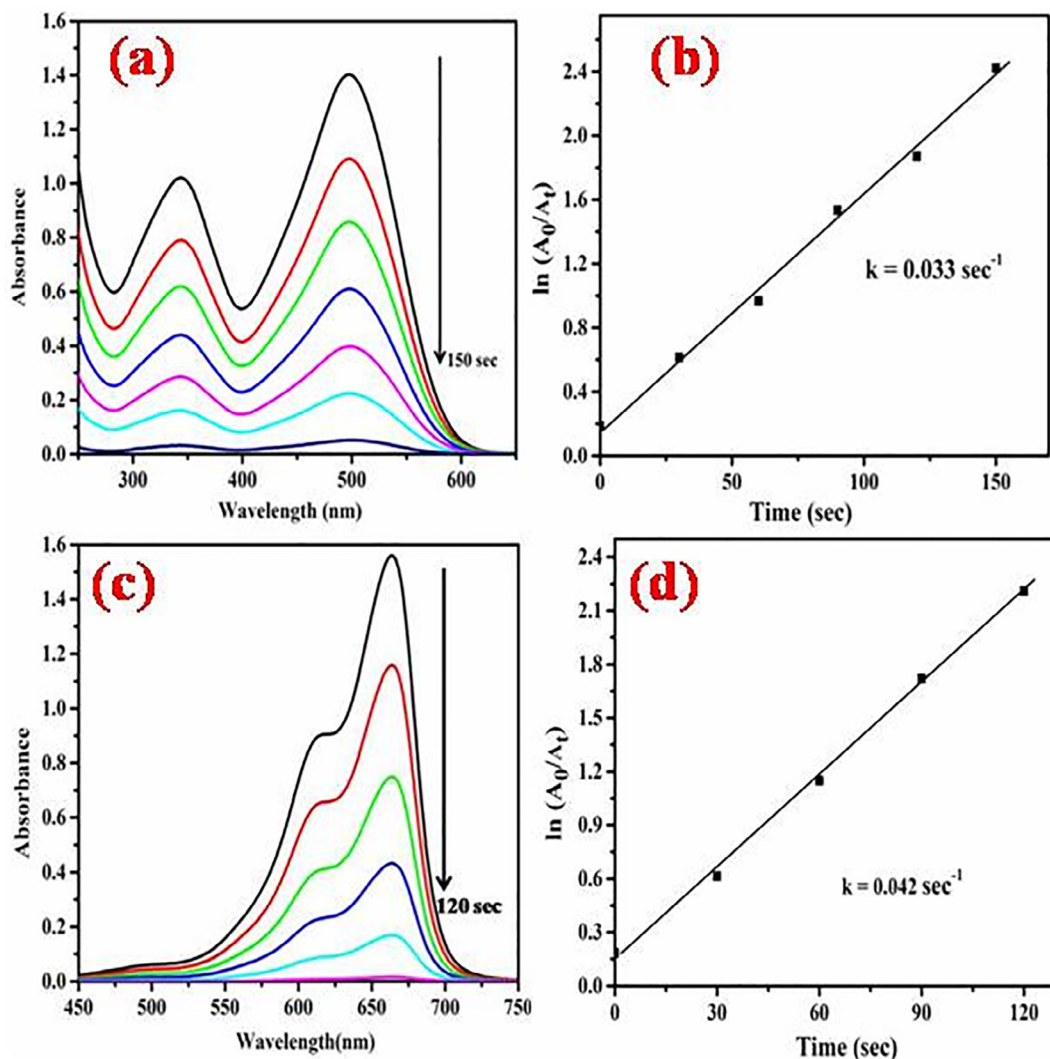
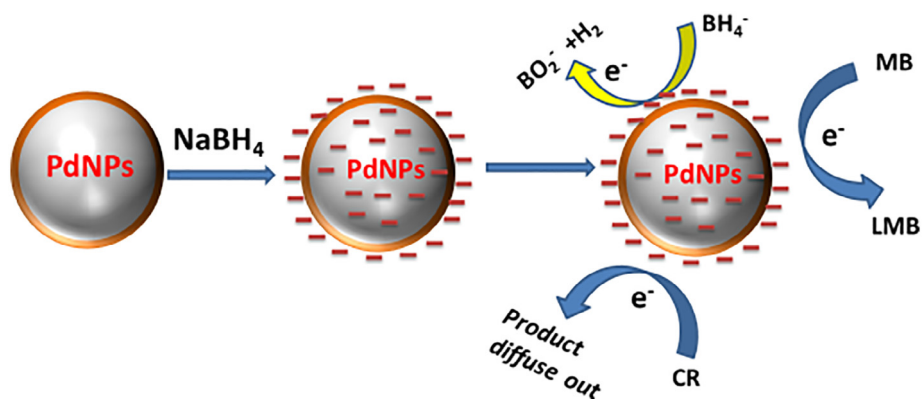


Fig. 1. (a) UV– Vis absorption spectra of resin, Pd<sup>2+</sup> solution and PdNPs, (b) FTIR (c) XRD and (d) TEM image of PdNPs.



**Fig. 2.** (a) Time dependent UV-Visible spectra of CR in the presence of PdNPs and (b) plot of  $\ln(A_0/A_t)$  vs time for the reduction of CR, (c) Time dependent UV-Visible spectra of MB in the presence of PdNPs and (d) plot of  $\ln(A_0/A_t)$  vs time for the reduction of MB.



**Fig. 3.** Schematic representation of the plausible mechanism for the  $\text{NaBH}_4$  mediated reduction of MB and CR  $\text{NaBH}_4$  by PdNPs.

found to be over 94%. Various kinetic models were applied to fit the data, and it was found that the plot of  $\ln(A_0/A_t)$  versus time (Fig. 2b) displayed linear correlation ( $R^2 = 0.99$ ) indicating the pseudo-first-order reaction kinetics and the rate constant was found to be  $0.033 \text{ s}^{-1}$  at room temperature (RT).

Fig. 2c shows the absorption spectrum of MB, that exhibit two absorption bands at 615( $n-\pi^*$ ) and 665 nm( $\pi-\pi^*$ ) characteristic to azo group [11]. Similar to CR, in the absence of PdNPs,  $\text{NaBH}_4$  alone was not able to reduce any significant portion of MB even after 100 min (Fig. S2). However, in the presence of PdNPs, MB

**Table 1**  
Comparison of the previous reported method with this work in the reduction of CR and MB.

	Catalyst	Time	Rate constant (k)	Reference
MB	AgNC	12 min	0.158 min <sup>-1</sup>	[11]
	salvia officinal AuNPs	10 min	0.112 min <sup>-1</sup>	[12]
	Salmalia-AuNPs	10 min	0.241 min <sup>-1</sup>	[13]
	Tragacanth/AgNPs	10 min	0.82 min <sup>-1</sup>	[14]
	HNTAgX	10 min	0.0016 s <sup>-1</sup>	[15]
	Pd-NanoCata	5 min	0.20 min <sup>-1</sup>	[6]
	<b>PdNPs</b>	<b>2 min</b>	<b>0.042 s<sup>-1</sup></b>	<b>This work</b>
CR	Salmalia-AuNPs	10 min	0.236 min <sup>-1</sup>	[13]
	Crocus Haussknechtii/AgNPs	9 min	0.011 s <sup>-1</sup>	[16]
	Sansevieria/AuNPs	8 min	0.331 min <sup>-1</sup>	[17]
	Dalspinin/AuNPs	8 min	0.004 s <sup>-1</sup>	[18]
	AgNPs/seashell	180sec	2.48 min <sup>-1</sup>	[19]
	<b>PdNPs</b>	<b>150 sec</b>	<b>0.033 s<sup>-1</sup></b>	<b>This work</b>

reduction was completed within 120 s. As shown in Fig. 2c, the intensity of absorption bands at 615 and 665 nm decreased rapidly. The efficiency of MB reduction was found to be over 94% and the plot of  $\ln(A_0/A_t)$  versus time (Fig. 2d) yield linear relation ( $R^2 = 0.99$ ) signifying the pseudo-first-order kinetics and the rate constant of 0.042 s<sup>-1</sup> was observed at RT. Possible mechanism of catalytic reduction is shown in Fig. 3 and explanation is provided in SI.

The catalytic efficiency of our PdNPs towards the reduction of MB and CR was compared with the previous reports (Table 1) and the results signified the superiority of our PdNPs. This improved efficiency can be ascribed to the efficient size control and stability provided by FR which in turn provides the large catalytic surface area. The reusability of PdNPs catalyst was checked for different cycles of CR, and MB reduction. At the end of each cycle, the catalyst was recovered by centrifugation, washed, dried and used for the next cycle. As shown in Figs. S3 and S4, very little catalytic activity loss after five cycles for the reduction reaction of CR and MB indicated the high stability of PdNPs.

#### 4. Conclusions

In summation, we have successfully developed a novel, rapid and inexpensive method for the preparation of PdNPs. Aqueous extract of *Frankincense* resin served both as reducing and stabilizing agent and microwave irradiation is employed. The PdNPs are crystalline and spherical in shape with an average diameter of  $11 \pm 2$  nm. PdNPs exhibited good catalytic properties for the reduction of CR, and MB. In addition, the PdNPs catalyst was recycled several times without significant loss of its catalytic activity. The ultra-fast catalytic degradation reactions followed a pseudo-first-order kinetics. High catalytic activity of PdNPs was ascribed to the efficient size control and stabilization effect of FR phytochemicals. Overall, this study explored the potential of FR in PdNPs preparation and paves the way for various other metal nanoparticles.

#### CRedit authorship contribution statement

**Kondaiah Seku:** Investigation, Writing – original draft, Funding acquisition. **Syed Sulaiman Hussaini:** Resources, Project administration. **Narasimha Golla:** Formal analysis, Data curation. **Girija Mangatayaru K:** Data curation, Visualization. **Sri Maha Vishnu D:** Formal analysis, Validation. **Rapolu Sridhar:** Validation, Data curation. **Rajkumar Bandi:** Data curation. **Bhagavanth Reddy G:** Conceptualization, Methodology, Supervision.

#### Declaration of Competing Interest

The authors declare that they have no known competing financial interests or personal relationships that could have appeared to influence the work reported in this paper.

#### Acknowledgment

Dr.Kondaiah Seku is thankful to The Research Council, Sultanate of Oman, for the financial support from TRC Research Grant (TRC Vide No.BFP/RGP/EBR/18/162).

#### Appendix A. Supplementary data

Supplementary data to this article can be found online at <https://doi.org/10.1016/j.matlet.2020.128427>.

#### References

- [1] D. Astruc, *Tetrahedron Asymmetry* 21 (2010) 1041–1054.
- [2] A. Paul, A. Paul, S. Yadav, *Tetrahedron Lett.* 61 (2020) 151364.
- [3] S. Ye, M. Yan, X. Tan, J. Liang, G. Zeng, H. Wu, B. Song, C. Zhou, Y. Yang, H. Wang, *Appl. Catal. B Environ.* 250 (2019) 78–88.
- [4] A. Bankar, B. Joshi, A. Ravi, S. Zinjarde, *Mater. Lett.* 64 (2010) 1951–1953.
- [5] S. Ye, G. Zeng, X. Tan, H. Wu, J. Liang, B. Song, N. Tang, P. Zhang, Y. Yang, Q. Chen, X. Li, *Applied Catal. B, Environ.* (2020) 118850.
- [6] V.J. Garole, B.C. Choudhary, S.R. Tetgure, D.J. Garole, A.U. Borse, *Int. J. Environ. Sci. Technol.* 16 (2019) 7885–7892.
- [7] S. Ye, G. Zeng, H. Wu, J. Liang, C. Zhang, J. Dai, *Resour. Conserv. Recycl.* 140 (2019) 278–285.
- [8] T. Morikawa, H. Matsuda, M. Yoshikawa, *J. Oleo Sci.* 66 (2017) 805–814.
- [9] B.R. Gangapuram, R. Bandi, M. Alle, R. Dadigala, G.M. Kotu, V. Guttena, *J. Mol. Struct.* 1167 (2018) 305–315.
- [10] V. Manikandan, P. Velmurugan, J.-H. Park, N. Lovanh, S. Seo, P. Jayanthi, Y. Park, M. Cho, B.-T. Oh, *Mater. Lett.* 185 (2016) 335–338.
- [11] P. Nariya, M. Das, F. Shukla, S. Thakore, *J. Mol. Liq.* 300 (2020) 112279.
- [12] M.H. Oueslati, L. Ben Tahar, A.H. Harrath, *Green Chem. Lett. Rev.* 13 (2020) 18–26.
- [13] B.R. Ganapuram, M. Alle, R. Dadigala, A. Dasari, V. Maragoni, V. Guttena, *Int. Nano Lett.* 5 (2015) 215–222.
- [14] M.K. Indana, B.R. Gangapuram, R. Dadigala, R. Bandi, V. Guttena, *J. Anal. Sci. Technol.* 7 (2016) 1–9.
- [15] T.K. Das, S. Ganguly, P. Bhawal, S. Remanan, S. Mondal, N.C. Das, *Appl. Nanosci.* 8 (2018) 173–186.
- [16] M. Mosaviniya, T. Kikhavani, M. Tanzifi, M. Tavakkoli, *Colloid Interface Sci. Commun.* 33 (2019) 100211.
- [17] I. Kumar, M. Mondal, V. Meyappan, N. Sakthivel, *Mater. Res. Bull.* 117 (2019) 18–27.
- [18] C. Umamaheswari, A. Lakshmanan, N.S. Nagarajan, *J. Photochem. Photobiol. B Biol.* 178 (2018) 33–39.
- [19] A. Rostami-Vartooni, M. Nasrollahzadeh, M. Alizadeh, *J. Colloid Interface Sci.* 470 (2016) 268–275.